PSIG 2205

Gas Pipeline Transient Modeling Via Transfer Functions: Field Data Validations

Cody Allen [1] *, *Roman Zamotorin* [1], *Avneet Singh* [1], *Rainer Kurz* [1]

[1] *Solar Turbines Inc., 4200 Ruffin Rd, San Diego, CA 92123, USA;*

** E-mail: allen_cody_w@solarturbines.com*

This paper was prepared for presentation at the PSIG Annual Meeting held in San Diego, California, 10 May – 13 May 2022.

ABSTRACT

Reduced order models, commonly referred to as ROMs, have been used in many areas of engineering due to their reduced complexity and corresponding speed of computation and solution. In transient pipeline simulation, transfer function-based ROMs have experienced widespread adoption spanning multiple decades due to their efficiency compared with higher order computational fluid dynamics. Many examples can be traced back to the 1980s Králik et. al. paper that considers simplified transfer functions. The choice of order of the simplified transfer functions then becomes the primary parameter that other authors amend compared with Králik. However, changing the order of the simplified transfer functions can have profound effects on the response of the system. Incidentally, it is necessary to understand the difference between true pipeline behaviors versus effects from the modeler's choice in further approximating the simplified transfer functions.

In this paper, we explore various simplified transfer function models and compare them with both a commercial grade modeling software and more importantly, with field data obtained from a large US based gas transmission pipeline. The field data validates certain model approximations and provides the modeling community a new set of high-resolution data that can be used for validating other models. We end the paper with an analysis and conclusion of how accurate the transfer function models were given the observed field data.

1 INTRODUCTION AND BACKGROUND

Pipelines are the most efficient method to transport energy over large distances. They produce the lowest amount of Greenhouse Gases over their life cycles when compared with Railway or Road based transportation [1] as well as being the safest method when comparing incident number and magnitude [2].

Many Natural Gas pipelines are operated under unsteady operating conditions, which in turn causes significant fluctuations in the operating conditions for the compressor stations in these pipelines. These fluctuations are the result of varying demand, as well as varying gas supply. For a given pipeline segment, the gas supply pressure and flow into the pipe are subject to change as are the pressure and flow demand on the delivery side of the pipe. These conditions, as well as their timing are only predictable to a degree.

The primary design criteria for pipeline networks is a specified flow capacity. Subsequent justification for pipeline installation cost and profitability around flow capacity utilizes steady state models [3]. These models allow definition of the required pipe diameters, distances between compressor stations, and power requirements for these stations. The simulation software has to be capable of accurately predicting pressure losses between stations based on the knowledge of gas compositions and temperatures, performance characteristics of the compressor trains, pipe geometry, pipe roughness, geography of the route and soil conditions.

In practice, interconnected gas pipelines rarely operate in steady state due to widely changing gas demand and dynamics introduced from injection and take off points along the pipeline. Recent geopolitical events involving Russia's attack on Ukraine have lead to massive uncertainty in natural

gas markets in Europe [4], causing scheduling conflicts and widely fluctuating supply and demand responses.

This unsteady nature of operation makes the use of reference data from steady state simulations difficult to use for modeling of a pipeline in transient operation. Consequently, steady state models are not ideal for depicting the time response of system upsets such as equipment failing or unscheduled load events along the pipeline. For these scenarios, dynamic or transient models are more useful and can give indications of how pressures and flows will evolve over a given time interval. However, these models are typically a type of *computational fluid dynamic* (CFD) model, which may utilize *Partial Differential Equations* (PDEs) or *Ordinary Differential Equations* (ODEs). The complexity of the models can result in large computational times, possibly so long that it renders the computation useless as the transient has come and gone by the time the simulation resolves. For this reason, a balance is needed between model accuracy and computational speed.

In this paper we examine transient simulations in the context of field data applied to State Space models. Then, we present two transient examples from an existing gas pipeline located in North America that occurred in October of 2021 and another in February 2022. We use part of the recorded field data as input into two transient models, one the authors have studied in a previous PSIG paper [5], which we refer to as the *simulation model* and one that is commercially available and well regarded in North America, *Synergi* [6]. The primary goal is to validate the simulation model from the authors' past paper compared with both commercial grade simulation software as well as actual observed data from the field. We end the paper with a discussion on the simulation model as well as future research topics based on these findings.

2 PIPELINE COMPRESSOR STATIONS

Compressor stations are the workers along the pipeline. As gas moves along the pipeline, energy is lost due to frictional effects. Compressor stations resupply energy to the gas to keep it flowing through the pipeline at the operator's required pressures and flow rates. The compressor station supplies this energy through the driver and gas compressor. Drivers are typically gas turbines, reciprocating diesel engines or electric motor drives. The compressors are usually centrifugal gas compressors or positive displacement compressors.

Gas turbine driven, variable speed compressors adapt to changing operating demands by controlling the power provided by the gas turbine, which primarily is set by the fuel flow into the combustor. A surrogate for the power produced by the turbine is the speed of its gas generator. The speed of the power turbine, and the gas compressor connected to it, are not controlled directly (as long as they stay within allowable ranges), but are established at the speed where the power produced by the power turbine is balanced by the power absorbed by the driven gas compressor.

If we consider the time scales between inputs and outputs of the system, we find degrees of separation. Specifically, a change in input at the driver fuel flow system occurs on the order of milliseconds to seconds and the corresponding response in output power occurs likewise. The driver as a whole then becomes the input to the gas compressor system, whose response to a change in inputs occurs on the order of seconds to minutes. Finally, the pipeline system, containing interconnected compressors and large segments of pipe, takes as inputs the various compressor stations' output, and whose response occurs on the order of hours and days.

For this reason, transient models at the pipeline system level typically neglect the gas turbine from the simulation, and focus on the response of the pressure and flow at the pipe inlet and outlets, using the combined responses from the gas turbines and corresponding responses from the gas compressors at the upstream and downstream compressor stations as the boundary conditions for the simulation [7, 8, 5].

Table 1 Data Collection Details

Data Sampling Period	10-minutes
Pressure Accuracy	$\pm 2.25\%$
Temperature Accuracy	$\pm 2.25\%$
Flow Rate Accuracy	$\pm 2.0\%$
Gas Chromatograph Accuracy	$\pm 0.5\%$

2.1 Data Collection

As a part of this work, we have collected data from two different transient examples that occurred on a North American pipeline. The data comes from a segment of the pipeline, namely, two separate compressor stations, connected by a single pipe. Figure 1 shows a block diagram of the system and the system boundary under consideration. Note that at both compressor stations there are two identical units in parallel configuration, where a gas turbine driving a high pressure centrifugal compressor is referred to as a *unit*.

Figure 2 shows a simplified schematic of the downstream compressor station. The circular elements represent various valves, where green indicates an open valve and red indicates a closed valve. In the figure, gas enters the compression station from the left (suction side) and flows out the right (discharge side). The trains shown represent a block for the combination of the gas turbine and compressor, what we refer to as a unit. Table 1 provides details on the data collected.

The two transient scenarios captured in the data are large pressure fluctuations. We present the transients on the compressor map in this section, then show individual outputs alongside the simulation outputs in the next section. Figures 3

and 4 show the transient in Example 1 at compressor stations N and $N+1$. In this case, we see the upstream unit follow an elliptic path during the transient. The downstream unit makes a nearly straight path down a constant efficiency contour and then returns back to its starting point.

Figures 5 and 6 show the transient in Example 2 again at compressor stations N and $N+1$. The downstream unit now takes a horizontal trajectory at the beginning of the transient and then moves into another straight line up and down, similar to Example 1. The initial horizontal trajectory is similar to those described in [9]. The upstream unit experiences some large fluctuations in flow rate at the 10-minute sampling level as indicated by large horizontal jumps on the compressor map during the middle of the transient. Eventually this behavior damps out and subtler movements prevail. Example 2 shows the need for faster sampling rates to better understand the dynamics of large flow rate and pressure changes.

3 INITIAL AND BOUNDARY DATA

The field data collected will be compared against the two different example simulations in this section. The first is the implementation of a *Transfer Function* based simulation of the *Navier-Stokes* equations. This model was presented in the authors' previous paper [5] where it was discussed how one can consider the friction factor as a tuning parameter instead of a value to be estimated by standard methods. Indeed, the friction factor plays in important role in simulation results as was shown previously. The simulation model is based on the work of Wen et. al. [10], where they further simplified work from Králik et. al. [11] and Behbahani-Nejad et. al. [7], into a *State Space* form. The second model is from the well known commercial software, Synergi [6]. We will start by presenting the results from the simulations for each example, then provide a discussion on parameters and assumptions. Note that while most values are presented in English Engineering physical units, all simulations of the authors' simulation model and supporting calculations are made in *SI* units, following the norm in the three primary reference papers [11, 7, 10].

Table 2 contains all constant values used in the simulations. Note that *dis* is short for discharge and similarly for suction and SS is short for *steady state*. Then, $P^{(N)}_{dis,ss}$ is the discharge pressure from compressor station N at steady state. The viscosity μ is taken from the NIST interactive charts [12] for Methane as the gas composition is approximately 96% Methane. Further, there is no appreciable elevation change between the two compressor stations. We follow the same format as previous authors for P_{0ss}, which is the steady state mean pressure between the two compressor stations. The mean temperature, T_{avg}, is the simple average whereas the mean pressure is calculated [13] by equation (3.1), applied to our scenario is given as:

Table 2 Simulation Initial and Boundary Conditions from Field Data

Constant	Sim. 1 Val.	Sim. 2 Val.
$P^{(N)}_{dis,ss}$	1225 [psig]	1212 [psig]
$P^{(N+1)}_{suc,ss}$	981 [psig]	1011 [psig]
P_{0ss}	1107 [psig]	1114 [psig]
Q_0	1315.7 [mmscfd]	1222 [mmscfd]
SG	0.5753 [1]	0.5753 [1]
MW	16.663 [lb/lbmol]	16.663 [lb/lbmol]
μ	8.62 $\times 10^{-6}$ [lbm/ft·s]	8.62 $\times 10^{-6}$ [lbm/ft·s]
T_{avg}	105 [$^\circ F$]	91.5 [$^\circ F$]
D	41.76 [inch]	41.76 [inch]
L	118.4 [mile]	118.4 [mile]
r	5.8$\times 10^{-4}$ [inch]	5.8$\times 10^{-4}$ [inch]

$$\frac{2}{3}\left(P^{(N)}_{dis,ss} + P^{(N+1)}_{suc,ss} - \frac{P^{(N)}_{dis,ss}P^{(N+1)}_{suc,ss}}{P^{(N)}_{dis,ss} + P^{(N+1)}_{suc,ss}}\right). \tag{3.1}$$

In order to run the simulation model, one chooses two outputs and two inputs from the list of inlet/outlet pressure and inlet/outlet mass flow. Recall, the model is based on deviations from the averaged steady state values [11, 7, 10] where Králik et.al. originally assumed all steady state pressures and mass flows were observable (known) prior to simulation. Behbahani-Nejad relaxed this requirement slightly, by only requiring a portion of values to be known prior to simulation, then used steady state hydraulic equations to calculate the remaining values. We follow this procedure in an effort to understand its validity for field data. Therefore, to implement the current simulation model, one is required to know the steady state pressures at both inlet and outlet, which are used in the calculation of P_{0ss}. Additionally, every so often, one must know the steady state outlet mass flow, which is calculated from knowing the steady state volumetric flow at standard conditions. This is only required when one is verifying the roughness value of the pipe segment, as we will explain later. When the roughness has been verified with data, knowing the steady state mass flow is no longer a necessary prior to simulation.

Once we have the values above the well known hydraulic general flow equation (3.2), is used to calculate Q_0,

$$Q_0 = 77.54D^{2.5}\left(\frac{T_b}{P_b}\right)\left(\frac{P_1^2 - P_2^2}{(SG)T_{avg}LZf}\right)^{0.5} \tag{3.2}$$

where $P_1 = P^{(N)}_{dis,ss}$ and $P_2 = P^{(N+1)}_{suc,ss}$ and units are as stated in equation (2.2) of [3]. With appropriate conversions applied to Q_0, one arrives at the required M_{0ss}.

For a given segment of pipe and during the initial simulation, we use field data to find the optimal pipe roughness value, r. The process is similar to that proposed in the authors' previous paper, however, for a single piece of pipe, the process was carried out manually and only involved two iterations. The process goes as follows: using SG, P_{0ss} and T_{avg}, one can find the *compressibility factor*, Z, and gas density, ρ, calculated using a model specifically for High Hydrocarbon Natural Gas [14],

$$Z = 1 + aP_{0ss} - b\frac{P_{0ss}}{T_{avg}} = \frac{1}{1 + \rho(b^* - a^* T_{avg})} \tag{3.3}$$

where $R_g \ [J/(kg \cdot K)] = \bar{R}/MW$, $a = 0.257/P_c$, $a^* = aR_g$, $b = 0.533T_c/P_c$, $b^* = bR_g$, $P_c = 4.64 \times 10^6 \ [Pa]$ and $T_c = 191 \ [K]$.

Once the average gas compressibility factor is estimated, the initial steady state standard flow calculated from (3.2) can be converted to a mass flow and the average *Reynolds* number and friction factor can be calculated. If the calculated standard flow does not match the observed steady state flow, the roughness value is changed, and the friction factor is recalculated and applied to (3.2). This process is repeated until the observed flow matches the calculated flow, where only the friction factor is changing in the iterations. Once the flow values converge, the estimated roughness value is set for all other transient simulations. At this point, the assumption of knowing the steady state mass flow is removed. Pipe internal roughness increases very slowly compared with transient fluctuations on the pipeline unless a specific event occurs that leads to an acute increase in the roughness. Therefore, once this value is found from an initial set of data, it can be used for many months thereafter. Finally, the average steady state gas velocity is calculated as a byproduct of calculating the Reynolds number.

The *Hofer* approximation [13] is used to calculate the friction factor. An interesting note is that when $Re \to \infty$, we have that $f \ \to \ \left(2\log_{10}\left(\frac{D}{r}\right) + 1.138\right)^{-2} = 0.0085$ in each example*. For comparison, in the first example, the friction factor is calculated to be 0.0088 with a Reynolds number of 2.841×10^7 and in the second example, the friction factor is calculated to be 0.0089 with a Reynolds number of 2.639×10^7. Using the steady state flow values in the second simulation applied to equation (3.2), with all other variables unchanged, the friction factor of 0.0089 produces a flow of 1217.45 [MMSCFD] vs the limiting friction factor of 0.0085 which produces a flow of 1245.77 [MMSCFD], a difference of approximately 2.27%. The high Reynolds number of gas flows† in pipelines and the low pipe roughness found in large gas transportation pipes enables the use of such approximations for the friction factor while limiting the error introduced.

Constant since it only depends on pipeline geometry in the limit.

†*Primarily due to the significantly smaller viscosity compared with liquids, which has more of an effect than the lower density.*

4 RESULTS AND DISCUSSION

In both examples, the black curve represents the authors' simulation model, the red curve is the Synergi output and the light blue curves are the field data.

The simulation results of Example 1 are presented in Figures 7 and 8. The simulation model stems from equations (31) and (32) in [10] but uses the updated model from the authors' paper [5], where equations (7) through (18), and the corresponding state matrices are used and where small errors in the Wen model have been fixed. In both simulations, the inputs u and outputs y are:

$$u = [\Delta P_{in} \quad \Delta M_{out}]^T \tag{4.1}$$

$$y = [\Delta P_{out} \quad \Delta M_{in}]^T. \tag{4.2}$$

with $\Delta P_{in} = P^{(N)}_{dis,obs} - P^{(N)}_{dis,ss}$ and $\Delta M_{out} = M^{(N+1)}_{obs} - M_{0ss}$. To recover the actual output values from the deviation outputs of y, we add back the steady state values: $P_{out} = \Delta P_{out} + P^{(N+1)}_{suc,ss}$ for simulated outlet pressure and $M_{in} = \Delta M_{in} + M_{0ss}$ for simulated inlet mass flow. Note that $M^{(N+1)}_{obs}$ is the observed, steady state mass flow at compressor station $N+1$ and similarly for compressor station N.

There are two immediate conclusions from the results:

1. The simulation model predicts the response reasonably well.
2. The model smoothes out variation in the response.

4.1 Simulation model vs Field Data vs Synergi

The authors were very pleased to see the responses matched the field data as well as they did. In Example 1, both predicted outputs experience a "transient to the transient", observable in the first three hours. We expect this initial departure comes from the deviation constants being different from the starting values of the predicted outputs. Faster sampling rates and correspondingly, higher frequency input data should cause this initial departure to take much less time to converge.

The predicted inlet flow ended up being higher than the field data, on average, about 15 mmscfd higher than observed. The Synergi model also had higher predicted values on average as seen in Figure 8. Attempts to remove this offset proved unfruitful. Slightly perturbing the steady state pressures and mass flow had very little effect on the predicted output. Furthermore, perturbations to the friction factor had a damping effect on the response: the higher the friction factor, the closer to a nearly horizontal line the response becomes, in both pressure and flow.

In Example 2, the tracking with field data was much closer and the constant offset was not observed. There were some impulse like sections of the field data that the model did

not fully capture, between 30 and 40 hours. Interestingly, the Synergi model over predicted the biggest impulses, but was quite close in general. It is also noteworthy that the "transient to the transient" was much smaller in this example as compared with the first example.

Some error may be attributed to the sampling period being too long. Králik et. al. did note in the original model assumptions that the maximum sampling period should be 600 seconds or 10 minutes, which is what our field data, and correspondingly, model input data is sampled at. We believe Králik selected this time based on the *Nyquist Rate* of the celebrated *sampling theorem* [15]. In reviewing the plots in [11], Figure 6 shows frequency domain plots from the longest pipe considered, a 31 mile pipe, where the characteristic frequency shown on each plot is $\omega = 0.005$ rad/sec. The subplot of interest is for transfer functions F_{P_2,M_2}, where the ordinate axis has a scale on magnitude 5×10^5. The graphic is too small to tell at what frequency ω^* the condition $X(j\omega) \approx 0$. Assuming Králik's selection was the value indicated on each plot, $\omega^* = 0.005$, the corresponding period length of the signal would need to be $\pi/0.005 \approx 628 \quad [sec] > T$, and rounding down to 600 [sec] gives the 10-minute threshold cited.

In both cases it is clear the that simulation model does not capture the higher frequency elements of the field data whereas Synergi captures some of the higher frequencies. This smoothing effect is a result of the modeling decision made by Wen et. al. in developing the state space model. The choice to make a *strictly proper*, second order transfer function [16] imposed a low pass filter onto the model output, which precisely manifests as a smoothing effect. That is, it filters out higher frequency elements from the input signals. One could certainly bring back the higher frequency deviations by choosing a higher order model and ensuring the model was not strictly proper, as was done originally by Králik et. al.. The authors plan to do this in future research.

A *Bode* plot is presented in Figure 11 and indicates precisely what frequencies can pass through the simulation model into the predicted outputs. Note that In(1) = $u_1 = \Delta P_{in}$ and In(2) = $u_2 = \Delta M_{out}$. Similarly, Out(1) = $y_1 = \Delta P_{out}$ and Out(2) = $y_2 = \Delta M_{in}$. A few interesting takeaways are:

1. u_2 dominates the output response of the model for both y_1 and y_2. Said another way, the outlet flow has a much more significant impact on both the predicted outlet pressure and inlet flow.
2. The frequency $f = 10^{-4}$ is the frequency at which u_2 starts becoming attenuated by the model.

In looking at the frequency $f_c = 10^{-4}$, we find the approximate transition point or *cutoff frequency* of the model. Since the model is parameterized for time units in seconds, we have

$$\begin{aligned} f_c = \frac{1}{per} &< 10^{-4} \ \ [sec] \\ \Leftrightarrow per &> \frac{1}{10^{-4} \ \ [sec]} = 10^4 \ \ [sec] \\ &\approx 2.78 \ \ [hour]. \end{aligned}$$

Therefore, if $u_2 \approx \sum_{i=1}^{N} A_i \sin(2\pi f_i t) + B_i$, then only frequencies such that $f_i < 10^{-4}$ for each $i = 1, 2, ..., N$ will have an effect on the predicted outputs. Higher frequencies are attenuated by the model. Lastly note, if one is running these simulations numerically, the combination of t and f must be set such that *signal aliasing* does not occur, otherwise the output will appear to pass higher frequency data, which is only an artifact.

5 CONCLUSION

In this paper we have attempted to validate the simulation model based on transfer functions formulated in state space form with two different observed transient response field data sets. The model performed admirably in both cases, although left some room for improvement. In particular, eliminating the constant offset of the predicted mass flow in Example 1 and better predicting the higher frequency signal content in both examples would be welcome improvements. Additionally, removing the initial prediction deviation or at a minimum, categorizing a time after which the model should track reality is needed. However, these are minor concerns compared with the utility of the current predictions, especially considering the speed of computations, less than one second on a standard laptop.

In future work we plan to derive our own transfer functions and corresponding state matrices, where the transfer functions are left proper, not strictly proper, which should help better capture higher frequency data fluctuations. It may also prove beneficial to re-examine the model assumptions and specify stricter requirements and assumptions if they further reign in deviations from the field data. Finally, we plan to investigate larger transients, such as unplanned shutdowns, and the model's ability to predict the corresponding responses.

ACKNOWLEDGMENTS

The authors would like to thank Solar Turbines Inc. for funding and supporting this research. We also thank Zachary Wilson for his guidance with the project.

REFERENCES

[1] B. Nimana, A. Verma, G. Di Lullo, M. M. Rahman, C. E. Canter, B. Olateju, H. Zhang, and A. Kumar, "Life cycle analysis of bitumen transportation to

refineries by rail and pipeline," *Environmental science & technology*, vol. 51, no. 1, pp. 680–691, 2017.

[2] D. Furchtgott-Roth, "Pipelines are safest for transportation of oil and gas," tech. rep., Manhattan Institute for Policy Research, 2013.

[3] E. S. Menon, *Gas Pipeline Hydraulics*. CRC Taylor and Francis Group, 2005.

[4] ZeroHedge, "Gas prices in europe skyrocket again as supply risks grow," 2022. https://oilprice.com/Energy/Natural-Gas/Gas-Prices-In-Europe-Skyrocket-Again-As-Supply-Risks-Grow.html (visited: 2022-03-07).

[5] C. W. Allen, C. Holcomb, R. Zamotorin, and R. Kurz, "Optimal Parameter Estimation for Efficient Transient Pipeline Simulation," vol. All Days of *PSIG Annual Meeting*, 05 2021. PSIG-2118.

[6] DNV, "Synergi pipeline simulator," 2022. https://www.dnv.com/software/services/pipeline/synergi-pipeline-simulator-index.html (visited: 2022-03-07).

[7] M. Behbahani-Nejad and Y. Shekari, "The accuracy and efficiency of a reduced-order model for transient flow analysis in gas pipelines," *Journal of Petroleum Science and Engineering*, vol. 73, no. 1-2, pp. 13–19, 2010.

[8] J. Fang, Q. Zeng, X. Ai, Z. Chen, and J. Wen, "Dynamic optimal energy flow in the integrated natural gas and electrical power systems," *IEEE Transactions on Sustainable Energy*, vol. 9, no. 1, pp. 188–198, 2017.

[9] R. Kurz and K. Brun, "Process control for compression systems," in *Turbo Expo: Power for Land, Sea, and Air*, vol. 50961, p. V009T27A001, American Society of Mechanical Engineers, 2017.

[10] K. Wen, Z. Xia, W. Yu, and J. Gong, "A new lumped parameter model for natural gas pipelines in state space," *Energies*, vol. 11, no. 8, p. 1971, 2018.

[11] J. Králik, P. Stiegler, Z. Vostrú, and J. Závorka, "Modeling the dynamics of flow in gas pipelines," *IEEE transactions on systems, man, and cybernetics*, no. 4, pp. 586–596, 1984.

[12] NIST, "NIST thermophysical properties of methane," 2022. National Institute of Standards and Technology; U.S. Department of Commerce; https://webbook.nist.gov/cgi/fluid.cgi?ID=C74828&Action=Page (visited: 2022-03-07).

[13] A. Fügenschuh, B. GeiRler, R. Gollmer, A. Morsi, M. Pfetsch, J. Rövekamp, M. Schmidt, K. Spreckelsen, and M. Steinbach, "Physical and technical fundamentals of gas networks," in *Evaluating Gas Network Capacities* (T. Koch, B. Hiller, M. Pfetsch, and L. Schewe, eds.), pp. 17–43, Mathematical Optimization Society - Society for Industrial and Applied Mathematics, 2015.

[14] F. M. White, *Fluid mechanics*. Tata McGraw-Hill Education, 1979.

[15] A. V. Oppenheim, A. S. Willsky, and S. H. Nawab, *Signals & systems*. Prentice Hall, 2 ed., 1997.

[16] M. de Oliveira, *Fundamentals of signals and systems*. Draft, 2021.

APPENDICES

The data sets presented in this paper can be downloaded at https://insightplatform.com/resources/resources/documents.html#technicalpapers.

AUTHOR BIOGRAPHIES

Cody Allen - is a Consulting Data Scientist in the InSight Analytics group at Solar Turbines Incorporated in San Diego, California. He is currently responsible for research and development of pipeline modeling software for transient simulation and mathematical optimization. Dr. Allen attended the University of California, San Diego where he received is Ph.D. in Mechanical Engineering and was awarded the Robert Skelton Systems and Controls Dissertation Award. He also holds a Masters degree in Applied Mathematics from San Diego State University, where he was awarded the Academic Excellence Award for Graduate Mathematics.

Roman Zamotorin - is a Consulting Engineer, Systems Analysis, at Solar Turbines Incorporated in Houston, Texas. He holds a doctoral degree from Saratov State Technical University, Russia and is responsible for performance evaluation and modeling of gas turbines and gas compressors, as well as for modeling pipelines. He is a frequent contributor to the PSIG conferences.

Avneet Singh - is the Manager, Systems Analysis at Solar Turbines Incorporated, in San Diego, California. His organization is responsible for predicting compressor and gas turbine performance, for conducting application studies, and for field performance testing. He holds a Bachelors Degree in Mechanical Engineering from University of California, San Diego.

Rainer Kurz - is the Manager, Gas Compressor Engineering at Solar Turbines Incorporated, in San Diego, California. His organization is responsible for the engineering of centrifugal gas compressors, including Design, Aerodynamics, Rotordynamics, Stress, and Advanced Products. Dr. Kurz attended the Universitaet der Bundeswehr in Hamburg.

FIGURES

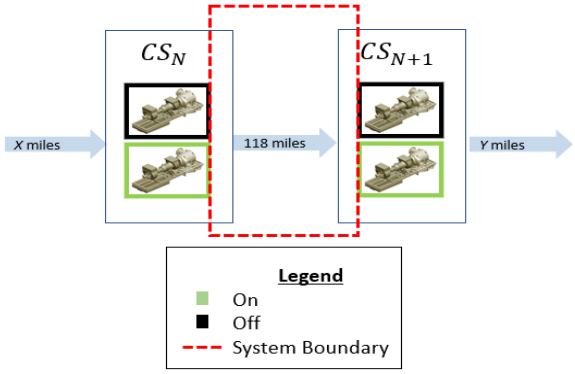

Figure 1: Field setup for data collection and simulation.

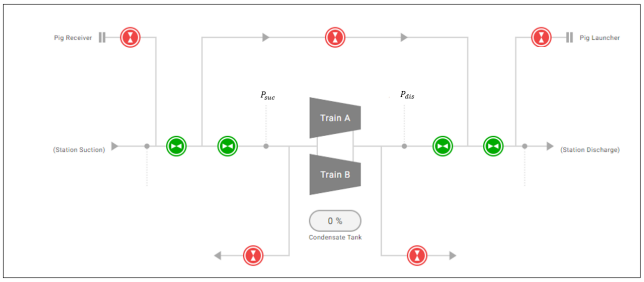

Figure 2: Simplified schematic for the downstream compressor station. Green valves represent open whereas red valves represent closed.

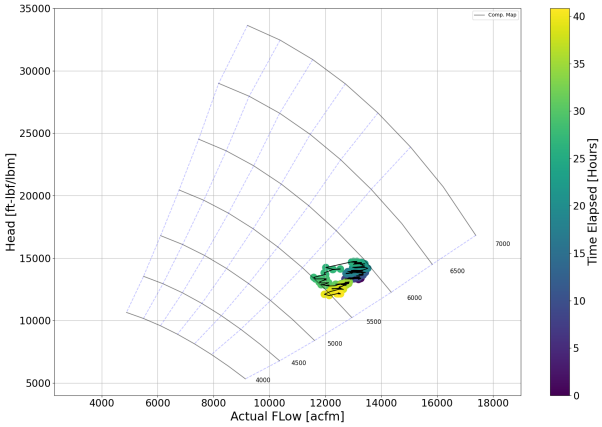

Figure 3: Upstream compressor station (CS_N) transient data for Example 1. The color of the points represents the passage of time, and the thin black connecting lines show the trajectory of the points.

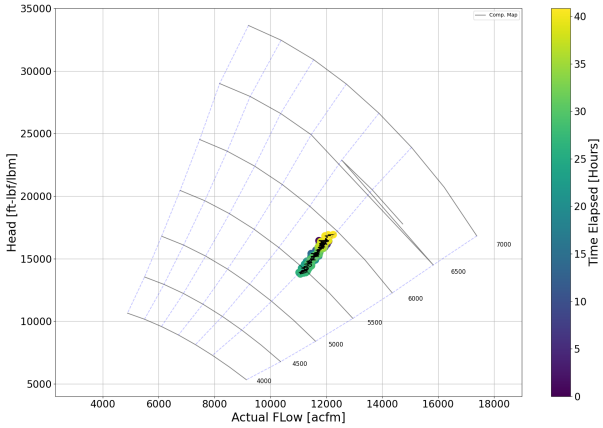

Figure 4: Downstream compressor station (CS_{N+1}) transient data for Example 1. The color of the points represents the passage of time, and the thin black connecting lines show the trajectory of the points.

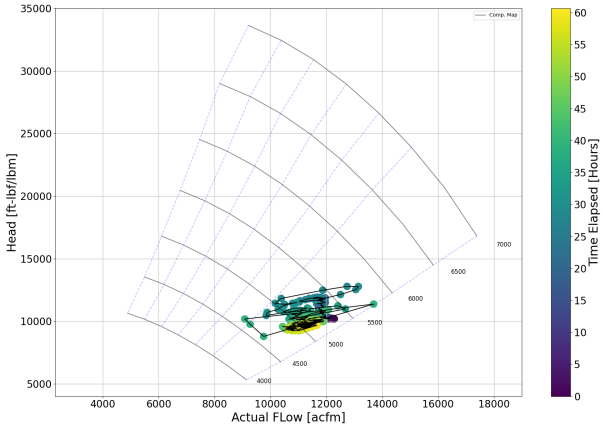

Figure 5: Upstream compressor station (CS_N) transient data for Example 2. The color of the points represents the passage of time, and the thin black connecting lines show the trajectory of the points.

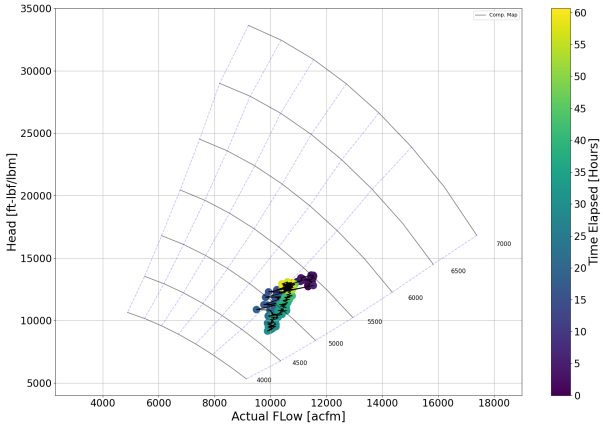

Figure 6: Downstream compressor station (CS_{N+1}) transient data for Example 2. The color of the points represents the passage of time, and the thin black connecting lines show the trajectory of the points.

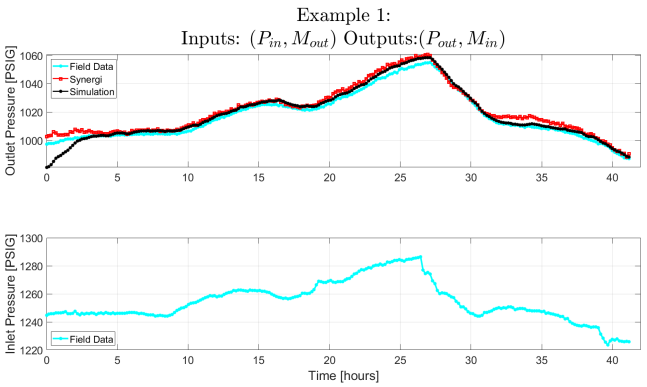

Figure 7: Simulation results for Example 1. Top: predicted CS_{N+1} outlet pressure. Bottom: Field data CS_N inlet pressure.

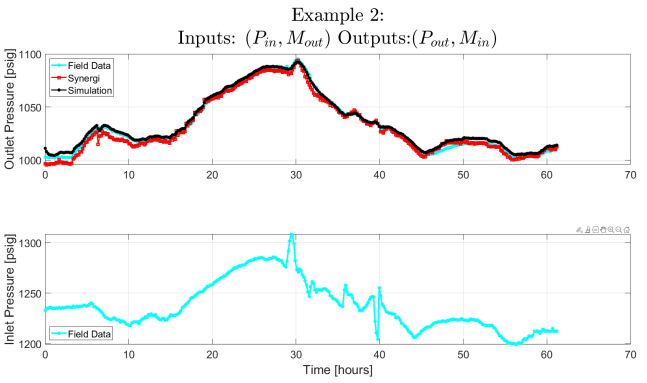

Figure 9: Simulation results for Example 2. Top: predicted CS_{N+1} outlet pressure. Bottom: Field data CS_N inlet pressure.

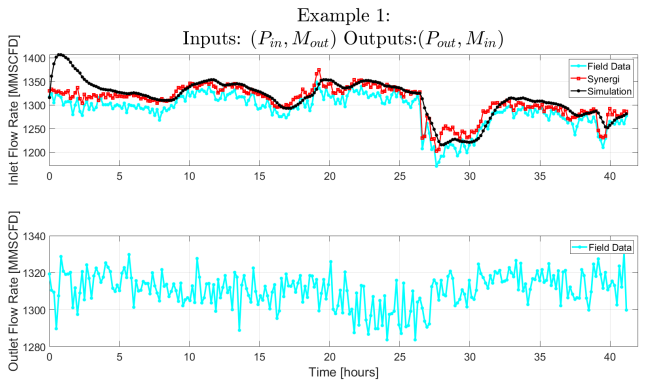

Figure 8: Simulation results for Example 1. Top: predicted CS_N inlet flow. Bottom: Field data CS_{N+1} outlet flow.

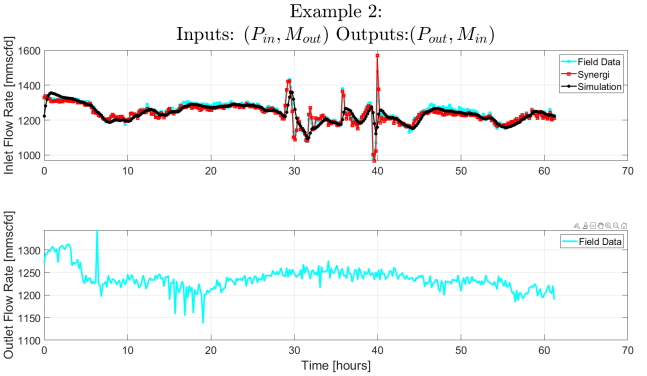

Figure 10: Simulation results for Example 2. Top: predicted CS_N inlet flow. Bottom: Field data CS_{N+1} outlet flow.

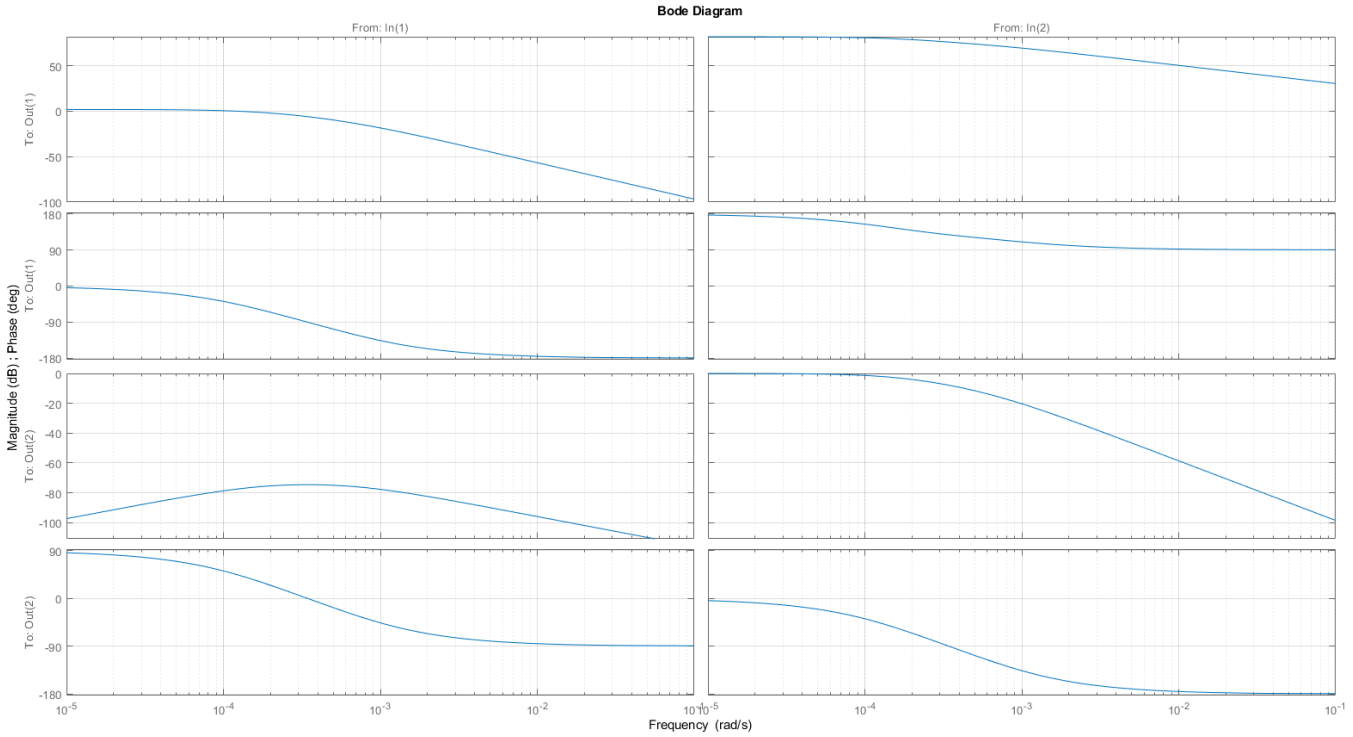

Figure 11: Bode Diagrams for the inputs to outputs in the State Space simulation model.